Vol. 33: 143–157, 2007 | CLIMATE RESEARCH Clim Res | Published February 22

Hydrologic impacts of climate change in the Upper Clackamas River Basin, Oregon, USA

David Graves, Heejun Chang*

Department of Geography, Portland State University, 424 Cramer Hall, Portland, Oregon 97201, USA

ABSTRACT: The Pacific Northwest of the USA is dependent on seasonal snowmelt for water resources that support its economy and aquatic ecosystems. Increased temperatures resulting from higher concentrations of atmospheric greenhouse gases may cause disruptions to these resources because of reductions in the annual snowpack and the earlier occurrence of seasonal snowmelt. We applied a Geographic Information System (GIS)-based distributed hydrologic model at a monthly scale to assess the effects of future climate change on runoff from the Upper Clackamas River Basin (UCB; located near Portland, Oregon, USA). Once validated using historic flow data, the model was run for 2 future time periods (2010–2039 and 2070–2099) using climate change simulations from 2 global circulation modelling groups (HadCM2 from the Hadley Centre for Climate Prediction and Research, and CGCM1 from the Canadian Centre for Climate Modelling and Analysis) as inputs. The model runs projected that mean peak snowpack in the study area will drop dramatically (36 to 49% by 2010–2039, and 83 to 88% by 2070–2099), resulting in earlier runoff and diminished spring and summer flows. Increases in mean winter runoff by 2070–2099 vary from moderate (13.7%) to large (46.4%), depending on the changes to precipitation projected by the general circulation models (GCMs). These results are similar to those of other studies in areas dependent on snowpack for seasonal runoff, but the reductions to snowpack are more severe in this study than in similar studies of the entire Columbia River Basin, presumably because the elevations of much of the Upper Clackamas Basin are near the current mid-winter snow line.

KEY WORDS: Oregon · Climate change · Geographic Information System · GIS · Hydrology · Model · Simulation · Runoff

1. INTRODUCTION

In the Pacific Northwest of the USA, increasing temperatures caused by the anthropogenic release of greenhouse gases will likely disrupt water resources during the 21st century because of reductions in the annual snowpack and the earlier occurrence of annual snowmelt. Even small increases in temperatures may have a significant effect on the timing of runoff, particularly in areas of moderate elevation near the current mid-winter snow line (Mote et al. 2003). Regonda et al. (2005) found that over the past 50 yr, peak spring flows have been occurring earlier throughout the Western United States, and have advanced most in mountainous areas of the Pacific Northwest below 2500 m, where winter temperatures are close to the melting point. Recent assessments for the Columbia River Basin portend significant disruptions to the economy and ecosystems that rely on seasonal water supplies under several climate change scenarios (Hamlet & Lettenmaier 1999, Miles 2000, Mote et al. 2003, Payne et al. 2004, Service 2004). These simulations project an increasing stress on water management systems and difficult tradeoffs between ecological uses (such as salmon migration) and economic uses (such as irrigation and hydropower production) under a warming climate. Hydrologic modelling offers a means to simulate the effects of climate change in order to better anticipate its effect on discharge quantity and timing from a watershed.

This study applied a hydrologic model to assess the effects of 21st century climate change on the hydrology of the Upper Clackamas River Basin (UCB), which is located southeast of Portland, Oregon, in the USA.

*Corresponding author. Email: changh@pdx.edu

This assessment complements other climate change studies of larger basins of the Pacific Northwest. The model uses a spatially distributed approach, which considers the heterogeneous characteristics of the watershed and models key hydrological processes throughout the study area. We used a modified soil water balance model—originally designed by Knight et al. (2001)—at a monthly scale with 1 km grid cells to simulate the effects of climate change on the timing and quantity of runoff from the UCB. Geographic Information System (GIS) data including climate, soil, and land cover data were used as inputs, and historic flow data and snow measurements were used to calibrate the performance of the hydrologic model over a contemporary period (1971 to 1985). Once calibrated, we validated the model for a subsequent period (1986 to 2000) using goodness-of-fit statistical methods. The validated model was run for 2 future time periods (2010–2039 and 2070–2099) in order to simulate the impacts of climate change on monthly discharge. We used projections of climate change from 2 general circulation models (GCMs; Hadley Center's IPCC-HadCM2GSAX 2005, available at http://ipcc-ddc.cru.uea.ac.uk/download_data/is92/hadcm2/HHGSAX61.zip; and the Canadian Centre for Climate's IPCC-CGCM1GSAX 2005, available at http://ipcc-ddc.cru.uea.ac.uk/download_data/is92/cccma/CCGSAX61.zip) run with IS92 (published in the 1992 supplementary Report to the IPCC Assessment) emission scenarios.

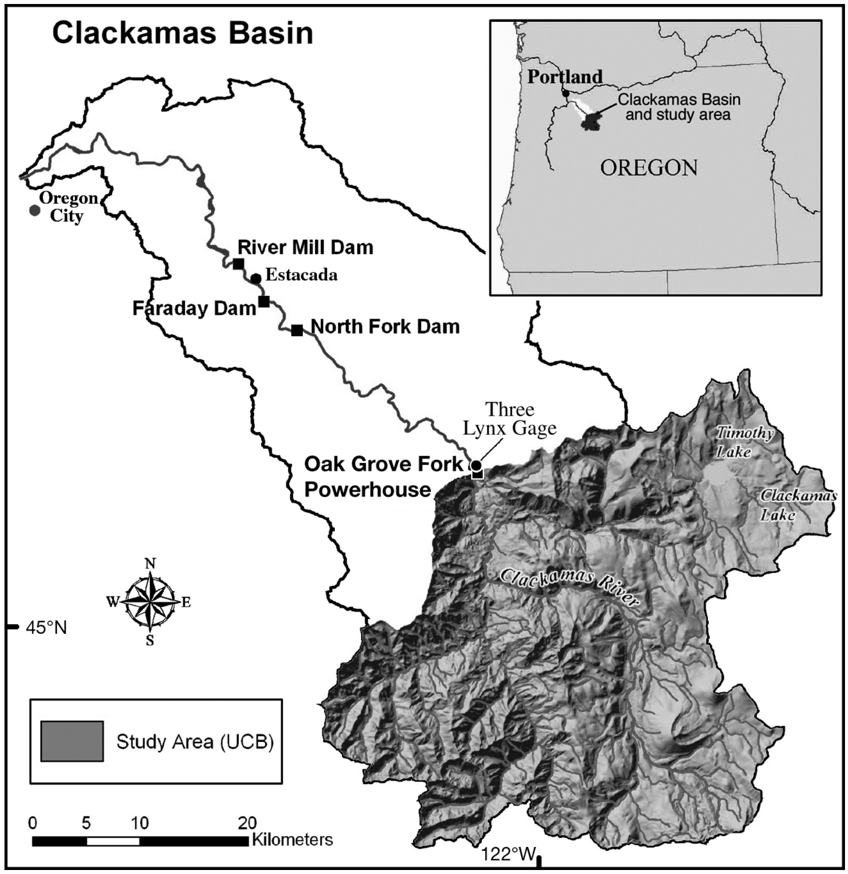

Fig. 1. Clackamas River Basin and study area. UCB: Upper Clackamas Basin

2. STUDY AREA DESCRIPTION

This study considers the upper half of the Clackamas River Basin (1260 km^2 of a total basin size of 2430 km^2) (Fig. 1). This includes the entire catchment located above the Three Lynx flow gage, which was used for model calibration and validation[1]. This area lies at moderate elevations (335 to 2197 m)[2].

The UCB is located on the western slopes of the Cascade Mountains, and its geology and soils are primarily influenced by processes in these mountains. The Cascade Mountains are composed of recently active volcanoes along the Cascade Crest to the east (the High Cascades), and older, inactive mountains to the west (the Western Cascades). The UCB contains about equal portions of both geologic areas. The Western Cascades are steep and well-eroded with shallow subsurface confining layers, while the High Cascades form a broad volcanic platform underlain by highly porous and permeable volcanic layers (Ingebritsen et al. 1992). Tague & Grant (2004) found that flow patterns of streams here are correlated with their underlying geology, with greater summer base flows and less seasonal variation occurring in High Cascades areas because of the larger role of permeable aquifers. In the Western Cascades, they found the opposite conditions with lower summer flows and greater seasonal variation because of impermeable soils and a well-developed drainage network.

Seasonal temperature fluctuations (Fig. 2) in the UCB are moderated by its proximity to the Pacific Ocean (~150 km) and the barrier influence of the Cascade Mountains against low continental temperatures during the winter (Dart & Johnson 1981). Despite these moderating effects, winter temperatures are usually

[1]Data available at http://waterdata.usgs.gov/or/nwis/si
[2]For further information see http://landcover.usgs.gov/natlandcover.asp

low enough to produce a significant snowpack. Between 1948 and 2000, mean winter month (December to March) temperatures measured at Estacada (Stn 352693) demonstrated a discernible warming trend (R^2 = 0.18), while April 1 snow water equivalent measured at Clackamas Lake (Stn 21D13) showed a declining trend (R^2 = 0.34) (Fig. 3).

The UCB receives an average of 195 cm of precipitation annually. Most of this precipitation is generated by frontal systems that arrive from the Pacific Ocean between October and May, and summers are generally dry (Fig. 2). Abundant precipitation feeds a dense network of streams, which are strongly influenced by melting snow during the winter and spring. The Oak Grove Fork watershed is regulated for hydropower production through managed releases from an earthen dam retaining Timothy Lake, while the Collowash and Upper Clackamas watersheds are free-flowing (Fig. 4).

The UCB is mostly forested and contains virtually no development aside from its road network, hydropower facilities, and a few residences. Approximately 29% of the UCB was harvested for timber between 1950 and 1994, but logging occurs at a slower pace today (Taylor 1999). Transitional areas that are regenerating compose about 5.9% of the UCB according to a 1992 land cover assessment (Table 1) (see footnote 2). Four dams on the lower Clackamas River (below the UCB) generate a total annual average of 758 million kWh of electricity, and the river is a municipal supply of water for approximately 175 000 people (data from www.portlandgeneral.com).

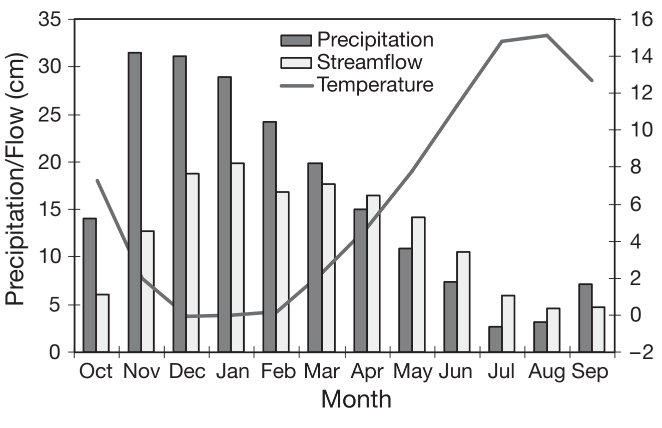

Fig. 2. Mean monthly temperature, precipitation, and discharge (flow) in the UCB from 1971 to 2000 (climate data from PRISM Model, www.ocs.oregonstate.edu/prism/index.phtml; see footnote 1 for discharge data)

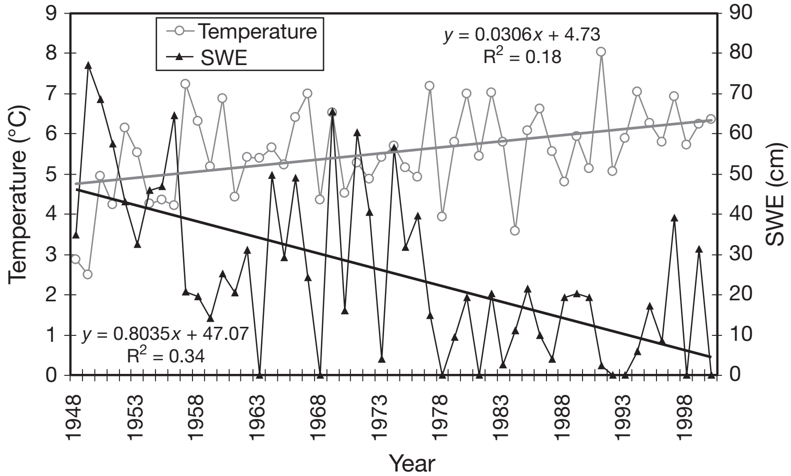

Fig. 3. Mean daily high temperature (December to March) and April 1 snow water equivalent (SWE) from 1949 to 2005, Estacada Climate Station (data from www.ocs.oregonstate.edu/index.html)

The UCB includes 3 runs of salmonids that are listed as threatened under the Endangered Species Act (see www.nwr.noaa.gov/salmon-habitat/critical-habitat/index.cfm).

The UCB was chosen for this study because of these important economic and ecological resources and because no assessment of climate change had been conducted there. It also warrants interest because its moderate elevations mean that it may be more susceptible to climate change than other basins located in higher areas in the Pacific Northwest of the USA.

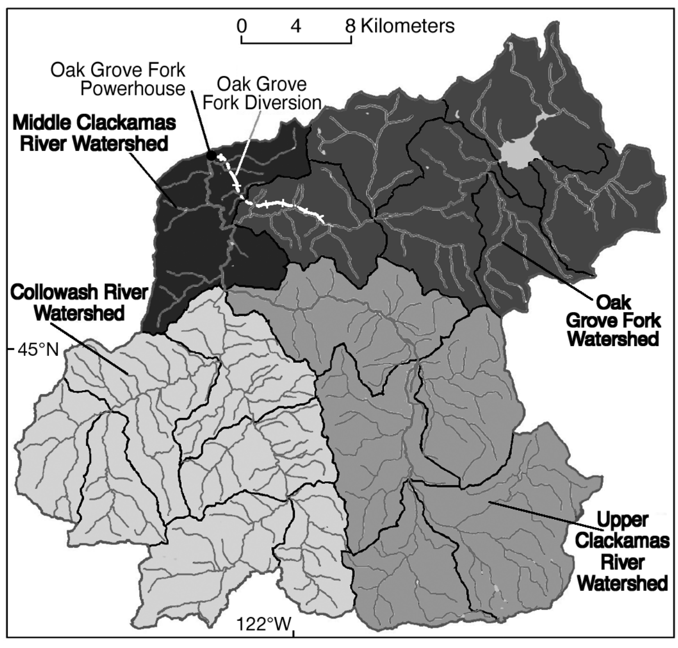

Fig. 4. Watersheds of the UCB (data from www.reo.gov)

Table 1. 1992 Land cover of Upper Clackamas River Basin (UCB) (data from USGS 1999)

Land cover	Proportion (%)
Evergreen forest	86.0
Barren/transitional	5.9
Mixed forest	2.8
Herbaceous upland	2.0
Shrubland	1.3
Deciduous forest	1.1
Open water	<0.1
Other	0.8

3. DATA AND METHODS

3.1. Input data

We used a modified version of a soil water balance model designed previously for the Struma River of Bulgaria. It is a conceptual, distributed model that approximates some of the physical processes of a watershed through monthly parameter-based operations on each pixel of a study grid (Knight et al. 2001, Chang et al. 2002). The Struma River model was chosen for this study following a literature review of hydrologic models used for similar assessments, because it met the following study objectives: (1) it is relatively simple and can be reconstructed from the scientific literature; (2) it is designed specifically with the intent to assess the effects of climate change with a fully distributed approach, using GIS data; (3) it is designed to work with monthly climate data.

The requisite climate data are total monthly precipitation, mean monthly temperature, and mean relative humidity data. A historical distributed monthly climate data set (Parameter–elevation Regression on Independent Slopes Model, PRISM), developed in 1994 by the Spatial Analysis Climate Service and the US National Resource Conservation Service (NRCS), provided historical and spatial climate data (temperature, precipitation, and dew point) necessary for the study inputs (Daly et al. 1994, 2002). PRISM data are organized in 2.5′ latitude/longitude grid cells, and contain climate estimates generated from measurements at nearby climate stations and a model of the orographic effects of the local terrain. We calculated relative humidity from dew point and temperature using Bolton's (1980) method (Table 2, Eq. 1).

Soil data (from the NRCS State Soil Geographic [STATSGO] soil database) were used to generate the maximum soil-moisture holding capacity for each cell,

Table 2. Equations used in the GIS-based distributed hydrologic model. PanEvap: pan evaporation, HoursDay: hours per day, Cof: coefficient

Equation	Formula	Source
(1) Computation of relative humidity from dew point	$E_s = 6.112 \times \exp[(17.67 \times T)/(T + 243.5)]$; $E = 6.112 \times \exp[(17.67 \times T_d)/(T_d + 243.5)]$; $RH = 100.0 \times (E/E_s)$ E_s: saturation vapor pressure in mb; E: vapor pressure in mb; T_d: dew point; T_a: temperature; and RH: relative humidity (%)	Bolton (1980)
(2) Estimation of monthly snowfall as % of precipitation	$\text{Snow}(\%) = 100/(1.35^T \times 1.61 + 1)$ T: monthly air temperature	Legates (1991)
(3) Linear degree day estimation of monthly snowmelt	$\text{Snowmelt (cm)} = \text{MRF} \times T \times \text{days in month}$ MRF: Melt rate factor (2.0 for forested areas, 3.0 for non-forested areas)	Kuchment & Gelfan (1996), Semadeni-Davies (1997)
(4) Estimation of monthly potential evaporation	$PE = -0.0018 \times (RH - 100) \times (T + 25)^2 \times \text{PanEvapCof} \times \text{HoursDayCof}$ PE: potential evaporation; PanEvapCof: 0.67; HoursDayCof depends on monthly fraction of annual hours of daylight in month	Knight et al. (2001)
(5) Adjustment of monthly potential evaporation by forest cover	$PE = PE \times (\text{fraction of forest}) + (1 - \text{fraction of non-forest}) \times 0.8$	Dunne & Leopold (1978)
(6) Estimation of actual evaporation	$AE = PE \times (SM/FC)$ if $SM \leq FC$ $AE = PE$ if $SM > FC$ AE: actual evapotranspiration SM: soil moisture; FC: field capacity	Knight et al. (2001)
(7) Estimation of monthly direct runoff	$DR = -0.095 + 0.208 \times \text{rainfall} / S^{0.66}$; $S = 1000/(SCN - 10)$ DR: direct runoff; S = potential maximum storage; SCN: soil curve number (derived from soil data)	Ferguson (1996)
(8) Estimation of monthly indirect runoff	$IR = (SM - FC) \times 0.31$ IR: indirect runoff	
(9) Estimation of monthly base flow	$BF = SM \times [0.13 + (FC - SM)/(FC \times 10)]$ BF: base flow	
(10) Estimation of monthly total runoff	$\text{Total runoff} = DR + IR + BF$	

which is necessary to calculate the soil moisture available for evaporation and runoff, and for use in determining the soil curve number for each cell, which affects infiltration rates (data available at www.ncgc.nrcs.usda.gov/products/datasets/statsgo/). We used 1992 National Land Cover Data (30 m resolution) to determine the soil curve number of each cell for infiltration capacity and other model processes that required forested cover (see footnote 2). We used a Digital Elevation Model (DEM) (also at 30 m resolution) to determine the mean elevation of each cell (available at http://seamless.usgs.gov/).

Data sets were downloaded in a GIS format and then projected onto a universal transverse mercator (UTM; Zone 10) coordinate system, clipped to the UCB boundaries, and intersected with a study grid to determine the characteristics of each cell of the grid. The study grid was generated by dividing the UCB area into 1 km^2 cells, producing a total of 1264 cells. Climate data were re-sampled at the finer 1 km^2 cell resolution of the study using a bilinear interpolation method. We moved all cell data into a relational database, and programmed the hydrologic model to run in this environment.

3.2. The distributed hydrologic model

This model uses the Thornthwaite water balance method (Thornthwaite 1955) to simulate monthly runoff and has 5 major components that approximate physical processes: (1) rain/snow; (2) snow cover and snowmelt; (3) infiltration/direct runoff; (4) soil moisture/evapotranspiration; and (5) indirect runoff. Table 2 gives the equations used in the model to produce the outputs of soil moisture, snowpack, evapotranspiration, and runoff for each cell during each month of the simulation. Fig. 5 shows the inputs, processes, and outputs of the final model used in this study; the structure of this model is somewhat different to that of the Struma River model structure (Knight et al. 2001) because of several modifications made to conform it to the conditions of the UCB.

We made modifications to this model during calibration in order to successfully simulate monthly flow. First, a rain-on-snow component was added to the model. In the Pacific Northwest, rain-on-snow melt events are often important contributors to winter flooding (Marks et al. 2001). Rainfall that occurs over snow was adjusted to run off rather than percolate into the snowpack, and was also assumed to 'force' the additional melting of a proportion of its volume from the snowpack. This proportion was added as a tuning variable, which is the ratio of rain-forced snowmelt to direct runoff. A multiplier of direct runoff for the months of December and January was added as an additional tuning variable for the model to approximate the increased flows from the UCB during these months. Direct runoff is determined in a large part by the intensity of rainfall: when a large quantity of precipitation falls over a short time, relatively less infiltration into the soil is likely to occur (Ferguson 1996). During the study period (1971–2000), December and January both received the greatest amount of average monthly precipitation and the most days with greater than 1 inch (2.54 cm) of precipitation. It is reasonable to assume that because the highest flows occur during December and January, more perennial streams may be active during this time and precipitation may enter the stream network more quickly, essentially occurring as increased direct runoff at the monthly scale.

To more closely approximate late summer flows, a second ground water component (base flow) was added to the model. With this modification, a proportion of surplus ground water still flows off each month as indirect flow, but a lesser proportion of soil moisture below the field capacity also discharges (base flow), contributing to the total flow from the basin (Table 2,

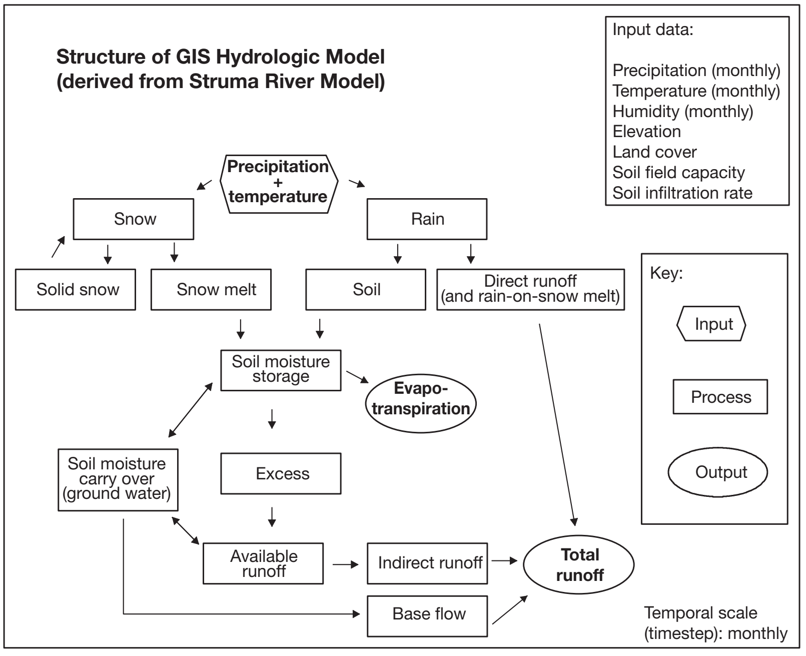

Fig. 5. Hydrologic model structure (modified version of diagram from Knight et al. 2001). GIS: geographic information system

Eq. 9). When the soil moisture is at or above field capacity, base flow occurs at an initial (minimum) proportion of the field capacity of the soil. When the soil moisture falls below field capacity, the base flow increases relative to the soil moisture (however, it decreases in absolute terms).

Indirect runoff and base flow were also modified to reflect differences in the underlying geology of the UCB described by Ingebritsen et al. (1992) and Tague & Grant (2004). All cells were grouped as part of the Western Cascades or the High Cascades. A geology coefficient was incorporated into the model, and during each month the indirect runoff and base flow quantities were calculated so that if a cell was part of the Western Cascades then its direct runoff was increased and its base flow was reduced, but if a cell was part of the High Cascades then its indirect runoff was reduced and its base flow was increased. The role of subsurface, permeable formations in recharging and sustaining base flow was therefore simulated in the High Cascades, and reduced in the relatively impermeable Western Cascades.

3.3. Model calibration and validation

The model was calibrated with historic stream flow data from the station above Three Lynx Creek on the Clackamas River (USGS gage No. 14209500). Flow data from this station were compared with modelled results to evaluate the effectiveness of runoff estimation. Historic measurements of snow water equivalent (SWE) conducted by the Oregon Snow Survey (available at www.or.nrcs.usda.gov/snow/) at the SNOTEL—SNOwpack TELemetry—sampling sites within the study area (Clackamas Lake, elevation 1037 m; Peavine Ridge, elevation 1067 m) were also compared with modelled predictions of SWE at their corresponding grid cell locations, but this was only used as a complementary method for calibration because of the differences in spatial and temporal scale between the modelled monthly grid data and the SNOTEL site measurements, which are measured at a specific point and time.

The model was 'tuned' with several goodness-of-fit measures during its calibration (Table 3). The deviation of runoff volumes (D_v) provides a simple measure of model performance and was the primary measure used. D_v measures the difference (%) between actual measured flow (AF) and modelled flow (MF) at Three Lynx Gage. The model was also calibrated according to its seasonal performance, using a monthly deviation (D_{vm}), and a Nash-Sutcliffe statistical test, which shows the difference in performance affected by small changes in the tuning parameters (Nash & Sutcliffe 1970). The final (calibrated) model performed well at representing monthly runoff from the UCB, with an average deviation from actual runoff of 16% (Table 3).

Table 3. Initial and final values of calibrated parameters for UCB with 1971–1985 data

Parameter	Value (Initial)	Value (Final)
Legates equation coefficient	1.61	1.61
Degree day melt rate coefficient	1.0	1.0
Pan evaporation coefficient	0.75	0.67
Direct runoff coefficient	1.0	1.0
Indirect runoff coefficient	0.20	0.31
Rain-on-snow coefficient	NA	3.0
Base flow coefficient (initial)	NA	0.13
Geology coefficient	NA	1.33
Dec/Jan direct runoff multiplier	NA	2.2
Results (1971–1985)		
Deviation of runoff volumes	33.2 (%)	16.0 (%)
Nash-Sutcliffe (mean annual flow)	0.48	0.84
Nash-Sutcliffe (mean monthly flow)	–0.04	0.67

The final model was validated using data from the second half of the study period (1986 to 2000). The measured and modelled monthly results were found to be normally distributed around their mean with the Kolmogorov-Smirnov goodness-of-fit (K-S) statistic. Multiple parametric statistical tests were used to provide a higher degree of confidence in the validation process: no one test is perfect for hydrologic assessments (ASCE Task Committee 1993, Legates & McCabe Jr. 1999). Table 4 summarizes the statistical tests and results used for this validation process.

The model performed fairly well at recreating flows from the basin over the validation period, explaining between 84 and 92% of the variability in the observed data when compared with an annual flow average, and 65% of the variability in the observed data when compared with monthly flow averages. These measures compare favorably with the results from some other hydrologic models (ASCE Task Committee 1993, Legates & McCabe 1999). Ideally, separate validations would be enlisted to evaluate the performance of the model in each of the watersheds of the study area and for each of the various model components, but the lack of available flow data do not make this feasible.

A brief sensitivity analysis of the tuning parameters was helpful to demonstrate their relative effect on the model performance. We adjusted each of the tuning parameters used for model calibration by +10, +20, –10, and –20% to determine their effect on overall monthly accuracy (D_{vm}), as well as on net runoff during the wet (October to March) and dry (April to September) seasons (Table 5). The model performance was most affected by the 2 parameters that control monthly

Table 4. Statistical tests used for validation of model with 1986–2000 data. MF: modelled flow; AF: actual observed flow; Av: average observed flow; Avm: average monthly observed flow; MAv: average modelled flow; n: no. of months

Statistical test	Equation	Description	Result
Mean absolute error (MAE)	$MAE = \Sigma\lvert AF - MF\rvert/n$	Absolute measure of model error in cubic meters per second	10.08 ($m^3\ s^{-1}$)
Deviation of runoff volumes (D_v)	$D_v = \left[\Sigma\lvert(AF - MF)/AF\rvert\right]/n$	Average difference (%) between measured and model flows	18.0 (%)
Pearson's coefficient of determination (R^2)	$R^2 = \frac{\left[\Sigma(AF - Av)(MF - MAv)\right]}{\left[\Sigma(AF - Av)^2\right]^{0.5}\left[\Sigma(MF - MAv)^2\right]^{0.5}}$	Standardized measure of model performance based on observed and predicted annual means (–1 to +1)	0.92
Nash-Sutcliffe coefficient of efficiency mean annual value (NS)	$NS = 1 - \frac{\Sigma(AF - MF)^2}{\Sigma(AF - Av)^2}$	Standardized measure of model performance against observed annual mean (–∞ to +1)	0.84
Nash-Sutcliffe coefficient of efficiency mean monthly values (NSm)	$NSm = 1 - \frac{\Sigma(AF - MF)^2}{\Sigma(AF - Avm)^2}$	Standardized measure of model performance against observed monthly means (–∞ to +1)	0.65

flow as a proportion of available water (the indirect runoff proportion, and the base flow proportion). Because the period of the sensitivity analysis (1971 to 2000) differed from that of the calibration period (1971 to 1985), some of the adjustments to parameters actually improved the overall performance of the model over the calibrated model.

Table 5. Results of sensitivity analysis (1971–2000). See Table 3 for definitions. D_v: deviation of runoff volumes

Run	Tuning parameter	Variation (%)	Mean monthly D_v (%)	Net D_v: wet season (%) (Oct–Mar)	Net D_v: dry season (%) (Apr–Sep)
1	CALIBRATED MODEL	NA	17.0	–0.9	2.0
2	RainOnSnowCof	+10	17.1	–0.2	1.0
3	RainOnSnowCof	+20	17.0	0.1	0.0
4	RainOnSnowCof	–10	17.2	–1.7	3.3
5	RainOnSnowCof	–20	17.4	–2.6	4.6
6	PanEvapCof	+10	16.9	–3.0	0.1
7	PanEvapCof	+20	17.1	–4.9	–1.8
8	PanEvapCof	–10	17.8	1.3	4.6
9	PanEvapCof	–20	19.2	3.6	7.3
10	IndirProp	+10	16.9	1.0	1.0
11	IndirProp	+20	17.0	2.0	0.0
12	IndirProp	–10	17.5	–2.5	3.4
13	IndirProp	–20	18.6	–4.2	4.9
14	BaseFlowProp	+10	17.8	–0.8	3.4
15	BaseFlowProp	+20	19.4	–0.5	4.8
16	BaseFlowProp	–10	17.2	–1.0	1.1
17	BaseFlowProp	–20	18.0	–1.0	0.2
18	DecJanMult	+10	17.0	–0.4	1.3
19	DecJanMult	+20	16.9	0.2	0.4
20	DecJanMult	–10	17.3	–1.5	3.1
21	DecJanMult	–20	17.5	–2.2	4.1
22	GeologyProp	+10	16.4	0.0	0.4
23	GeologyProp	+20	16.0	1.0	–1.8
24	GeologyProp	–10	17.9	–1.7	3.7
25	GeologyProp	–20	18.5	–2.5	4.9

3.4. Model application for climate change scenarios

The validated model was run with outputs from 2 GCM simulations—the Hadley Circulation IS92 Greenhouse Gas and Sulphate Ensemble Mean Model (IPCC-HadCM2GSAX 2005, hereafter HadCM2) and the Canadian Centre for Climate Modelling and Analysis IS92 Greenhouse Gas and Sulphate Ensemble Mean Model (IPCC-CGCM1GSAX 2005, hereafter CGCM1)—in order to simulate the potential effects of climate change on monthly temperature and precipitation (Johns et al. 1997, Flato et al. 2000). Although more recent data are available, we chose these simulations because they were used for the US National Climate Assessment and the Struma River Assessment that the hydrologic model initially was developed for (Chang et al. 2002[3]). GCMs from this series were also used in other assessments in the Pacific Northwest (Hamlet & Lettenmaier 1999, Miles et al. 2000). Therefore, in using these GCMs, we were able to directly compare our results with those from previous studies. Ideally, the model could be run with several additional scenarios; however, we were not predicting actual changes

[3]See also www.usgcrp.gov/usgcrp/nacc/default.htm

to flow but instead outlining various future possibilities, and these 2 scenarios show a wide range of potential change. These climate simulations project an effective greenhouse-gas-forcing change corresponding to a compounded increase in CO_2 at a rate of 1% yr^{-1}, and the reflection of incoming radiation by increased sulphate aerosols (Johns et al. 1997, Flato et al. 2000). These assumptions are derived from middle-of-the-road projections of 21st century population growth and fossil fuel use (IPCC 2001).

The hydrologic model was run for 2 time periods with each of the GCM simulations, 2010–2039 (hereafter referred to as the 2020s in this study, because it projects approximate climate during this decade) and 2070–2099 (hereafter referred to as the 2080s). The mean monthly projections of change in these 4 climate scenarios were used to adjust the monthly temperature and precipitation values of the 30 yr baseline period (1971–2000) and to project future climate change for the 2020s and 2080s. While macro-scale hydrologic models for large basins are often used in combination with GCMs, assessments for smaller basins generally use climatic outputs from GCMs, which may be downscaled to the scale of the study (Xu & Singh 2004).

We downloaded the temperature and precipitation model data for each of the climate simulations from the IPCC Data Distribution Centre (available at http://ipcc-ddc.cru.uea.ac.uk), and extracted the values for the grid cells that surround the UCB (Fig. 6). These grid cells are coarse (HadCM2: 3.75° longitude × 2.5° latitude; CGCM1: 3.75 longitude × 3.75 latitude), and no one cell represents the UCB well, so we interpolated the change values of the nearby cells (HadCM2: 6 cells; CGCM1: 4 cells) for each month with a kriging method using the GIS software to a half-degree cell resolution, and then calculated the mean values for the UCB. The kriging method, which takes into account spatial dependence, develops a prediction map based on the values of the nearby cells and is useful for downscaling precipitation and temperature data when spatial autocorrelation between nearby locations exists. Kriging is often recommended over interpolation methods because it uses a semivariogram (spatial model) of an entire area to produce more accurate results (Burrough & McDonnell 1998, Zimmerman et al. 1999).

The results project that mean annual temperatures in the UCB will increase by about 1.3°C by the 2020s and approximately 3.5°C by the 2080s (Table 6). Both GCM scenarios show mean annual precipitation increases of approximately 5.4% by the 2020s. However, they differ in their projections of precipitation increases by the 2080s; the HadCM2 simulation shows moderate annual increases (+12.4% by the 2080s), while the CGCM1 simulation shows large annual increases (+27.1% by the 2080s). Globally, precipitation may be expected to increase with rising temperatures because this will provide more energy for evaporation, but this is expected to vary locally. The distribution of increases in precipitation and evapotranspiration will likely drive local increases and decreases in river flows (Arnell 2003). The final validated hydrologic model was run with these adjustments to monthly temperature and precipitation for the 4 climate scenarios (HadCM2 2020s and 2080s, CGCM1 2020s and 2080s) and the baseline period (1971–2000).

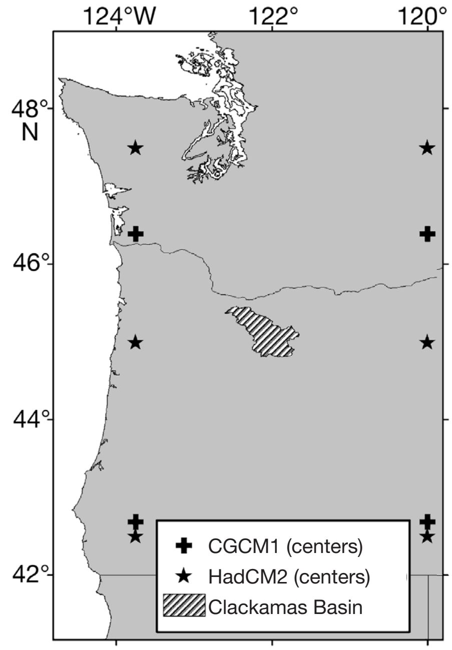

Fig. 6. Relative location of UCB and neighboring GCM grid cells

4. RESULTS

4.1. Annual effects of climate change

The hydrologic model projects that annual evapotranspiration in the UCB will show moderate increases by the 2020s and large increases by the 2080s (Table 7). The scenarios differ considerably by the 2080s: under the HadCM2 scenario, increased evapotranspiration negates all precipitation increases, and annual runoff volumes are unchanged from the 1971–2000 baseline period; under the CGCM1 scenario, a large increase in precipitation exceeds increased evapotranspiration, and annual runoff volumes are 20.8% higher than during the baseline period. In both scenarios, the proportion of precipitation falling as snow decreases significantly between the baseline period (26.5%) and the 2080s (HadCM2: 14.1%; CGCM1: 14.0%).

Table 6. Changes to mean monthly precipitation and temperatures of UCB from the HadCM2 and CGCM1 GCMs

Month	Precipitation (%)				Temperature (°C)			
	2025		2085		2025		2085	
	HadCM2	CGCM1	HadCM2	CGCM1	HadCM2	CGCM1	HadCM2	CGCM1
Jan	−0.5	+6.3	+11.4	+46.7	+1.6	+1.4	+3.6	+4.0
Feb	+6.5	+12.7	+13.8	+50.4	+1.6	+1.3	+3.5	+4.1
Mar	−3.8	+8.8	+1.6	+28.9	+1.4	+1.6	+3.0	+3.7
Apr	−1.7	−11.2	+1.3	−9.2	+1.2	+1.4	+2.9	+3.5
May	+7.3	−22.5	+21.9	−9.5	+0.8	+1.6	+2.1	+3.8
Jun	+14.5	−4.7	+9.5	+15.2	+1.3	+1.3	+3.3	+4.3
Jul	−7.1	−1.9	−4.7	+4.3	+1.4	+1.2	+3.8	+3.3
Aug	+19.8	+0.0	+2.5	+12.1	+1.2	+1.0	+4.5	+3.0
Sep	+2.9	+0.9	+6.8	+20.5	+1.7	+1.3	+4.3	+3.8
Oct	+24.7	−2.2	+55.0	+25.8	+0.9	+1.2	+2.4	+4.0
Nov	+12.9	+11.0	+10.9	+31.7	+1.1	+1.1	+2.8	+3.4
Dec	+2.7	+24.4	+9.4	+46.0	+1.5	+1.4	+3.6	+3.3
Yearly	+5.3	+5.5	+12.4	+27.1	+1.3	+1.3	+3.3	+3.7

Table 7. Modelled average annual precipitation, rainfall, snowfall, evapotranspiration and runoff for UCB under 5 climate-model/time periods. All units: cm

Period	Precipitation	Rainfall	Snowfall	Evapotranspiration	Runoff
Baseline, 1971–2000	194.8	143.2	51.6	46.0	148.5
CGCM1, 2020s	207.9	160.6	47.3	54.2	153.5
HadCM2, 2020s	205.4	162.2	43.2	55.2	150.0
CGCM1, 2080s	255.3	219.5	35.8	75.6	179.4
HadCM2, 2080s	218.9	188	30.9	70.1	148.5

4.2. Monthly changes to flow

Fig. 7 shows mean monthly flows under the baseline and future climate scenarios. During the 2020s, mean flows remain largely unchanged in both scenarios from the baseline period during October and November, but are greater during the winter months and reduced during the rest of the hydrologic year. These trends are more pronounced in the CGCM1 scenario than in the HadCM2 scenario, where both mean January flow increases from baseline (+16.4 vs. +9.8%) and mean July decreases from baseline (–16.3 vs. –15.3%) are greater. These trends are modelled to continue in the 2080s, with larger increases in baseline winter flows and larger decreases in baseline summer flows than in the 2020s simulations. The 2080s CGCM1 scenario shows larger increases in baseline winter flow than in the 2080s HadCM2 scenario (48.7 vs. +15.9% for Jan-

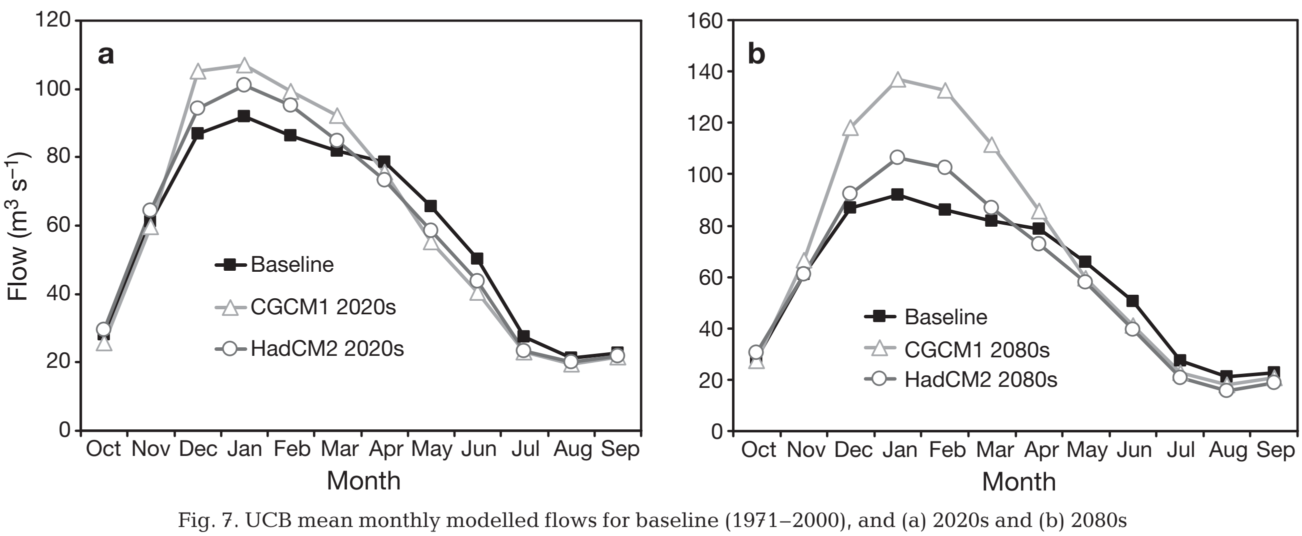

Fig. 7. UCB mean monthly modelled flows for baseline (1971–2000), and (a) 2020s and (b) 2080s

uary) but smaller reductions to baseline summer flow (–17.8 vs. –24.7 % for July), demonstrating the sensitivity of the hydrologic model to the larger precipitation inputs from the CGCM1 2080s data.

Interestingly, the month of peak runoff (January) remains unchanged in all of the climate scenarios. This seems to contradict the observed trends of earlier runoff that were recorded during the 20th century throughout the western United States (Regonda et al. 2005, Stewart et al. 2005). However, the peak in monthly runoff (January) differs from peaks in spring-onset melting, which are established in these research studies at a finer temporal scale but not adequately captured in the monthly data used in this study.

4.3. Seasonal changes to flow

While monthly change to flow from the entire UCB is important, in terms of water resource management it is also useful to anticipate where localized flows may change on a seasonal basis. Table 8 shows the projected change to baseline flow from each of the 3 major watersheds (Fig. 4) of the UCB during the annual periods of highest and lowest flow. During high flow months (December to February), all simulations predict that average flow will increase most from the Upper Clackamas watershed and least from the Collowash watershed. During low flow months (July to September), all simulations predict that flow will decrease most from the Oak Grove Fork watershed and decrease least from the Collowash watershed.

A relationship between changes to runoff and elevation is shown consistently in both scenarios during the wet season (October to March), but not during the dry season (April to September) (Tables 9 & 10). All model runs indicate a correlation between higher elevations and greater increases in wet season (October to March) runoff from the baseline period, presumably because of greater winter rainfall and reduced snowpack. During the dry season, the CGCM1 scenarios show a strong correlation between lower elevations and larger decreases in runoff in the 2020s and 2080s, but the HadCM2 scenario shows no clear relationship during the 2020s and a weaker opposite relationship during the 2080s, with larger decreases in dry season runoff from higher elevations. These differences may be accounted for by the variation in monthly precipitation changes between the HadCM2 and CGCM1 scenarios, which may offset the effect of a lower snowpack.

Table 8. Modelled flow change (%) from the baseline (1971–2000) by UCB watershed during high and low flow periods. See Fig. 4 for watersheds

Watershed	2020s		2080s	
	HadCM2	CGCM1	HadCM2	CGCM1
Change in mean flow during high runoff months (Dec–Feb)				
Collowash	7.6	16.9	11.1	45.2
Oak Grove Fork	13.3	20.7	18.2	51.7
Upper Clackamas	14.1	21.6	21.3	57.3
Change in mean flow during low runoff months (Jul–Sep)				
Collowash	–3.7	–5.7	–18.0	–9.5
Oak Grove Fork	–11.7	–12.8	–31.0	–18.8
Upper Clackamas	–10.6	–11.2	–27.9	–17.6

4.4. Monthly and seasonal changes to snowpack

All climate scenarios projected a significant reduction in annual snowfall, an acceleration of snowmelt, and a consequent decrease in monthly snow accumulation, measured as the average SWE of the UCB (Fig. 8). While mean SWE for the area is still projected to peak around the end of February in the 2020s, it drops from the baseline period by nearly half (CGCM1: 17.0 to 10.8 cm; HadCM2: 8.6 cm). The simulated decrease by the 2080s is even more dramatic: mean snowpack is projected to peak at only 2.9 cm around the end of December in the CGCM1 scenario, and at only 2.1 cm around the end of January by the Hadley scenario.

The spatial distribution of changes to snowpack is shown in Fig. 9. Modelled snowpack is generally greater in the high-elevation areas (>1200 m) to the east, particularly in the plateau area to the southeast, which in the contemporary period (1971–2000) is projected to retain a healthy snowpack (>12 cm SWE per cell) at the beginning of May during average years. The contemporary simulation also shows almost all of the UCB to be covered (>2 cm mean SWE per cell) with snow on March 1. The HadCM2 projection of snow distribution (Fig. 9a) shows very similar results for both periods. SWE decreases substantially in all of the scenarios, with the western half of the UCB losing virtually all of its snow accumulation and the eastern portions holding very little spring (May 1) snowpack by the 2080s. In the CGCM1 projection (Fig. 9b), the 2020s distribution of snowpack on March 1 is much diminished and, in the 2080s assessment, the March 1 snowpack is clearly reduced in most areas than the contemporary May 1 snowpack, signifying a dramatic transformation of the contemporary regime.

Table 9. Modelled seasonal runoff change (October–March/April–September, %) from the baseline (1971–2000) by elevation range

Elevation (m)	2020s CGCM1	2020s HadCM2	2080s CGCM1	2080s HadCM2
414–700	+11.8/–14.4	+6.1/–10.4	+37.2/–12.6	+8.3/–17.0
701–950	+13.1/–13.4	+7.7/–10.7	+38.5/–10.0	+10.2/–17.1
951–1200	+13.7/–12.4	+8.7/–10.6	+37.9/–6.8	+10.9/–16.9
1201–1450	+13.9/–12.2	+9.6/–11.0	+40.0/–6.9	+12.4/–17.6
1451–1871	+14.1/–9.6	+10.7/–9.9	+45.5/–7.0	+16.9/–19.1

Table 10. Pearson's correlation coefficients of modelled seasonal runoff change from baseline (1971–2000) to elevation. Seasons—wet: October–March; dry: April–September. *$p < 0.01$

Season	2020s CGCM1	2020s HadCM2	2080s CGCM1	2080s HadCM2
Wet	+0.17*	+0.32*	+0.17*	+0.28*
Dry	+0.21*	–0.04	+0.21*	+0.08*

5. DISCUSSION

This assessment foresees some clear changes in water balance in the hydrologic cycle that are likely to occur with 21st century climate change. Evapotranspiration is projected to increase and snowpack to diminish greatly, in a fairly uniform pattern. The Model predicts moderate reductions in spring and summer flows by the 2020s, and significant reductions by the 2080s. Increasing rainfall and snowmelt during both periods lead to higher flows during the winter months. During the 2020s, the scenarios are in fairly close agreement about the magnitude of these changes, but they diverge during the 2080s time period, primarily because of different projections of precipitation increases in the GCMs. In the CGCM1 2080s scenario, large increases in precipitation offset some of the losses to spring and summer runoff but are likely to bring very high flows during the fall and winter months. In the HadCM2 2080s scenario, precipitation increases are modest and winter increases in runoff are largely unchanged from the 2020s scenario, but reductions in spring and summer flow are severe. Annual runoff remains largely unchanged from the baseline period in all simulations except the CGCM1 2080 scenario, which projects it to increase substantially (+20.8%) because of greater annual precipitation inputs.

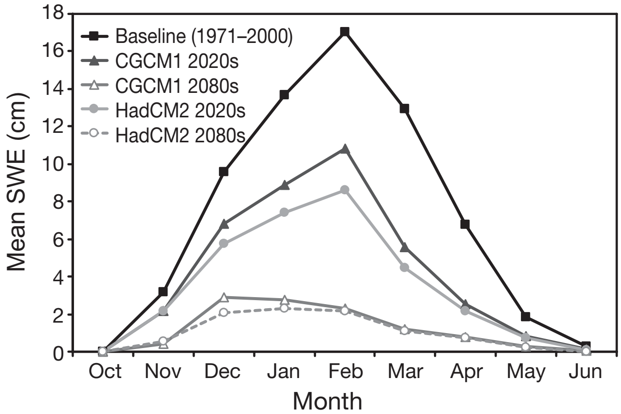

Fig. 8. Average modelled snow water equivalent (SWE) of the UCB under 5 scenarios

Spatially, these changes are more pronounced in the high elevation areas of the UCB (primarily to the east) that receive more runoff from snow. Of the 3 major watersheds, the Upper Clackamas appears most vulnerable to changes, both in the form of wet season flooding and dry season droughts. The Upper Clackamas watershed currently receives a large amount of its runoff from the snowpack and, unlike the Oak Grove fork watershed, it has no managed reservoirs that could be used to help mitigate the effects of a warmer climate.

The results of this study agree with the major findings of several other assessments of the hydrologic effects of climate change in snowmelt-dominated basins, which also project that warmer temperatures can be expected to reduce the snowpack in the future, leading to earlier seasonal runoff. These studies were conducted in locations as varied as the Swiss Alps (Seidel et al. 1998, Jasper et al. 2004), southern Germany and the central Alps (Kunstmann et al. 2004), the western Himalayas of India (Singh & Bengtsson 2004), a Mediterranean Basin (Chang et al. 2002), the Catskill Basin of New York (Frei et al. 2002), various mountainous basins throughout the western USA (Van Katwijk et al. 1993, Stonefelt et al. 2000), and in global assessments of snowmelt dominated areas (Arnell 2003, Barnett et al. 2005). While these studies are largely in agreement regarding a trend towards a reduced snowpack during the 21st century, they differ in their projections of the severity of disruptions to the timing and quantity of runoff, and whether annual runoff will increase or decrease.

These effects are largely dependent on physical variations among geographical areas, changes to precipitation during the 21st century, and the hydrologic model used in each study. In Frei et al.'s (2002) study in the Catskills, which also uses a Thornthwaite soil water balance approach, the authors found that the basin response to warmer temperatures will be largely dependent on precipitation changes. Stonefelt et al. (2000) came to similar conclusions in their study of a mountainous California watershed, determining that

Fig. 9. (This and facing page.) Modelled distribution of snowpack in the UCB for (a) HadCM2 and (b) CGCM1 scenarios

precipitation is most important for annual water yield, and temperature most important for the timing of streamflow.

The results of this study also generally agree with other assessments of the Pacific Northwest, with a few differences. Broad studies of the Columbia River Basin (Hamlet & Lettenmaier 1999, Payne et al. 2004) also foresee reduced snowpack and earlier runoff. Hamlet & Lettenmaier's (1999) study is especially useful for comparison with this study because it addressed similar periods (2020s and 2090s), using one of the same climate models (HadCM2) as an input. As with this study, it showed an increasingly early spring melt during the 21st century, but our reductions in peak (March 1) SWE in the UCB in the 2020s are larger (–49%) than those modelled by Hamlet & Lettenmaier (1999) for the entire Columbia Basin (–15%). This discrepancy can be attributed to the large proportion of the UCB that is at moderate elevations (98.5% of the UCB is located between 500 and 1700 m) compared with the Columbia Basin, which encompasses large areas at high elevations and with continental climates that may be less sensitive to small increases in temperature. The HadCM2 scenario in Hamlet & Lettenmaier's (1999) study also projected that winter runoff will increase while summer runoff decreases, but differs in projections of annual runoff (2020s, change to annual runoff: Hamlet & Lettenmaier +23% vs. UCB [present study] +1%; 2090s, change to annual runoff: Hamlet and Lettenmaier: +12% vs. UCB [2080s; present study] +0%).

While a comparison with these other studies reinforces our UCB findings, it is important to emphasize that our assessment is based on several assumptions and incorporates the results of GCMs that are complex and differ in their own assessments. The effects of climate change are uncertain because of complex interactions between earth and atmospheric systems.

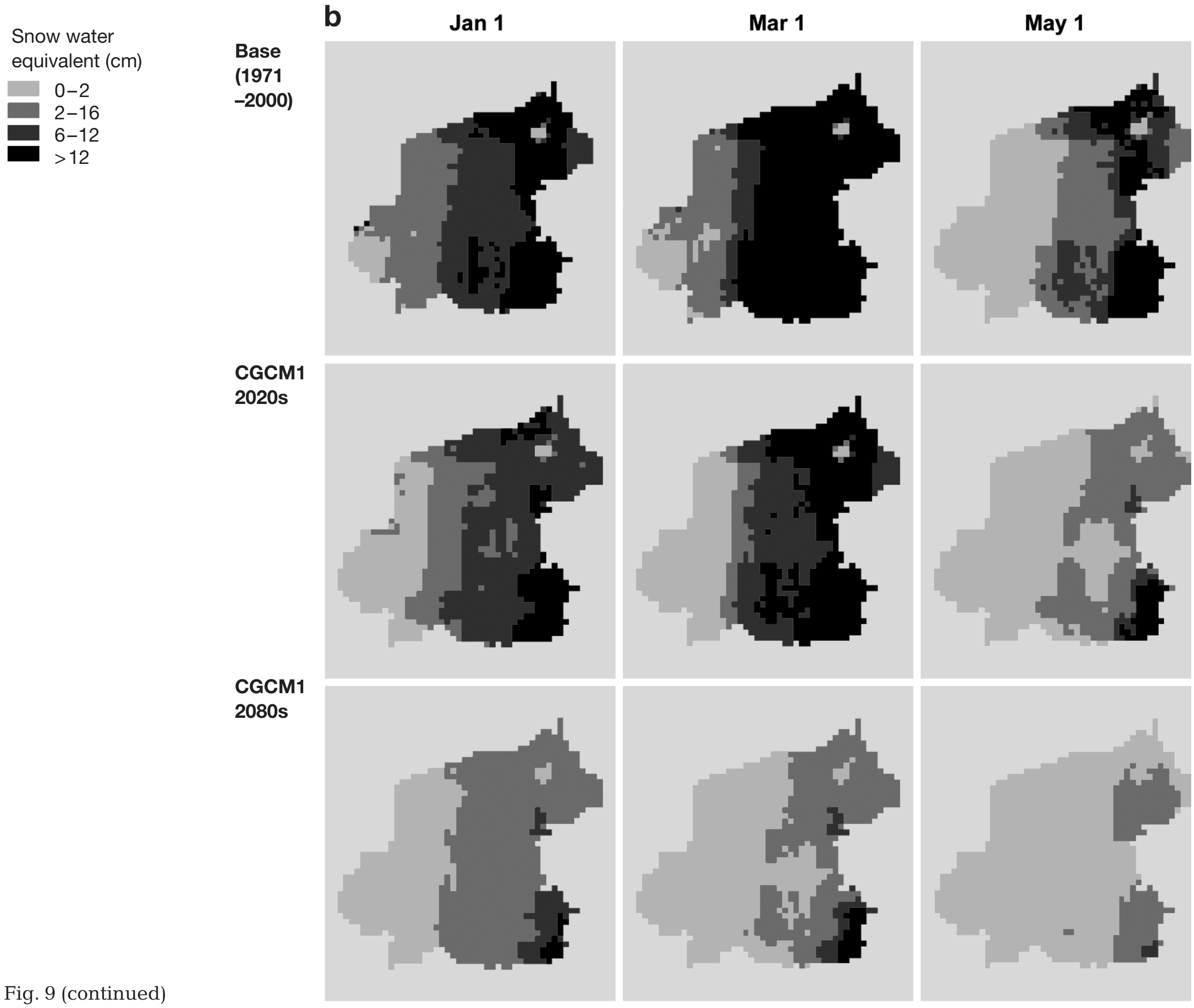

Fig. 9 (continued)

For example, a greater supply of CO_2 in the atmosphere can generally be expected to increase plant growth while decreasing transpiration, which might preserve more water for runoff (Wigley & Jones 1985). It is uncertain what this reduction would be and whether it would be offset by a coincident increase in canopy leaf area, or limited by available nutrients (Gifford 1988, Van Katwijk et al. 1993, Shelton 1999). Climate change may also be expected to change the composition of vegetation in the UCB in the long term and affect the frequency of forest fires (Mote et al. 2003). The effects of increased atmospheric aerosols on global temperatures are also uncertain, but probably unlikely to neutralize or reverse greenhouse warming (Barnett et al. 2005). Additionally, projections for certain time periods (2020s and 2080s) are based on a contemporary 30 yr period, and actual conditions during these periods will be influenced by climate variability, especially Pacific Decadal Oscillation and El Niño Southern Oscillation (ENSO) cycles, which are important drivers of river runoff in the Pacific Northwest of the USA and are expected to be so in the future (Mote et al. 2003, Beebee & Manga 2004, Stewart et al. 2005; see also footnote 3). The modelled approach used in this study did not attempt to incorporate these uncertain processes, but simply assumes that the anthropogenic release of CO_2 and other greenhouse gases will occur at the rate projected by the GCMs used in this study (a doubling by 2100) and that these global simulations are reliable predictors of local climate change. Hence, uncertainty remains until reliable regional climate models are developed (MacCracken et al. 2004).

Future opportunities for related research include the use of different GCM scenarios and other hydrologic models, which may simulate physical processes at varying temporal and spatial scales, to assess the impacts of climate change on the water resources of the UCB. Water resource managers would also benefit from applied studies that evaluate the consequences of anticipated changes to the quantities of seasonal flows on water resource uses of the Clackamas River. The most important applications of these studies would probably be for the in-stream uses of hydropower production, and for aquatic habitat in the area, particularly that of salmon, which have been listed under the Endangered Species Act of 1973.

Acknowledgements. We appreciate constructive comments from the editor and 3 anonymous reviewers. Thanks also to the Oregon Water Resources Office of the USGS for providing assistance and reference materials for this study. This research was supported by a Faculty Enhancement Grant at Portland State University. Additional support was provided by a grant (Code No. 1-9-2) from Sustainable Water Resources Research Center of the 21st Century Frontier Research Program in Korea.

LITERATURE CITED

Arnell NW (2003) Effects of IPCC SRES emissions scenarios on river runoff: a global perspective. Hydrol Earth Syst Sci 7:619–641

ASCE Task Committee (1993) Criteria for the evaluation of watershed models. J Irrig Drain Eng 1193:429–443

Barnett TP, Adam JC, Lettenmaier DP (2005) Potential impacts of a warming climate on water availability in snow-dominated regions. Nature 438:303–309

Beebee RA, Manga M (2004) Variation in the relationship between snowmelt runoff in Oregon and ENSO and PDO. J Am Water Resour Assoc 40:1011–1024

Bolton D (1980) The computation of equivalent potential temperature. Mon Weather Rev 108:1046–1053

Burrough PA, McDonnell RA (1998) Principles of geographical information systems. Oxford University Press, New York

Chang H, Knight CG, Staneva M, Kostov D (2002) Water resources impacts of climate change in southwestern Bulgaria. Geojournal 57:115–124

Daly C, Neilson RP, Phillips DL (1994) A statistical-topographic model for mapping climatological precipitation over mountainous terrain. J Appl Meteorol 33:140–158

Daly C, Pasteris P, Gibson WP, Taylor GH, Johnson GL (2002) A knowledge-based approach to the statistical mapping of climate. Clim Res 22:99–113

Dart JO, Johnson DM (1981) Oregon: wet, high, and dry. The Hapi Press, Portland, OR

Dunne T, Leopold LB (1978) Water in environmental planning. WH Freeman, New York

Ferguson B (1996) Estimation of direct runoff in the Thornthwaite water balance. Prof Geogr 48:263–271

Flato GM, Boer GJ, Lee WG, McFarlane NA, Ramsden D, Reader MC, Weaver AJ (2000) The Canadian centre for climate modelling and analysis global coupled model and its climate. Clim Dyn 16:451–467

Frei A, Armstrong RL, Clark MP, Serreze MC (2002) Catskill Mountains water resources: vulnerability, hydroclimatology, and climate-change sensitivity. Ann Assoc Am Geogr 92:203–224

Gifford RM (1988) Direct effects of CO_2 concentrations on vegetation. In: Pearman GI (ed) Greenhouse: planning for climate change. CSIRO, Melbourne

Hamlet AF, Lettenmaier DP (1999) Effects of climate change on hydrology and water resources in the Columbia River Basin. J Am Water Res Assoc 35:1597–1623

Houghton JT, Ding Y, Griggs DJ, Noguer M, van der Linden PJ, Xiaosu D (eds) (2001) Climate change 2001: the scientific basis. Contribution of Working Group I to the Third Assessment Report of the Intergovernmental Panel on Climate Change (IPCC). Cambridge University Press, Cambridge

Ingebritsen SE, Sherrod DR, Mariner RH (1992) Rates and patterns of groundwater flow in the Cascade Range volcanic arc, and the effect on subsurface temperatures. J Geophys Res 97:4599–4627

Jasper K, Calanca P, Gyalistras D, Fuhrer J (2004) Differential impacts of climate change on the hydrology of two alpine river basins. Clim Res 26:113–129

Johns TC, Carnell RE, Crossley JF, Gregory JM, Mitchell JB, Senior CA, Tett SB, Wood RA (1997) The second Hadley Centre coupled ocean-atmosphere GCM: model description, spinup, and validation. Clim Dyn 13:103–134

Knight CG, Chang H, Staneva M, Kostov D (2001) A simplified model for simulating runoff: the Struma River GIS. Prof Geogr 53:532–543

Kuchment LS, Gelfan AN (1996) The determination of the snowmelt rate and the meltwater outflow from a snowpack for modelling river runoff generation. J Hydrol 179: 23–36

Kunstmann H, Schneider K, Forkel R, Knoche R (2004) Impact analysis of climate change for an alpine catchment using high resolution dynamic downscaling of ECHAM4 time slices. Hydrol Earth Syst Sci 8:1030–1044

Legates D (1991) An evaluation of procedures to estimate monthly precipitation probabilities. J Hydrol 122:129–140

Legates D, McCabe G (1999) Evaluating the use of 'goodness-of-fit' measures in hydrologic and hydroclimatic model validation. Water Resour Res 35:233–241

MacCracken M, Smith J, Janetos AC (2004) Reliable regional climate model not yet on horizon. Nature 429:699

Marks D, Link T, Winstral A, Garen D (2001) Simulating snowmelt processes during rain-on-snow over a semi-arid mountain basin. Int Glaciol Soc 32:195–202

Miles E, Snover A, Hamlet A, Callahan B, Fluharty D (2000) Pacific Northwest regional assessment: the impacts of climate variability and climate change on the water resources of the Columbia River Basin. J Am Water Resour Assoc 36:399–420

Mote PW, Parson EA, Hamlet AF, Keeton WS and 7 others (2003) Preparing for climate change: the water, salmon, and forests of the Pacific Northwest. Clim Change 61: 45–88

Nash JE, Sutcliffe JV (1970) River flow forecasting through conceptual models. J Hydrol 10:282–290

Payne JT, Wood AW, Hamlet AF, Palmer RN, Lettenmaier DP (2004) Mitigating the effects of climate change on the water resources of the Columbia Basin. Clim Change 62:233–256

Regonda KS, Rajagopalan B, Clark M, Pitlick J (2005) Seasonal shifts in hydroclimatology over the Western United States. J Clim 18:372–384

Seidel K, Ehrler C, Martinec J (1998) Effects of climate change on water resources and runoff in an alpine basin. Hydrol Proc 12:1659–1669

Semadeni-Davies A (1997) Monthly snowmelt modelling for large-scale climate change studies using the degree day approach. Ecol Model 101:303–323

Service R (2004) As the West goes dry. Science 303: 1124–1127
Shelton ML (1999) Climate change and future hydroclimate for the upper Crooked River, Oregon. Phys Geogr 20: 14–26
Singh P, Bengtsson L (2004) Hydrological sensitivity of a large Himalyan basin to climate change. Hydrol Proc 18: 2363–2385
Stewart IT, Cayan DR, Dettinger MD (2005) Changes toward earlier streamflow timing across western America. J Clim 18:1136–1155
Stonefelt M, Fontaine T, Hotchkiss R (2000) Impacts of climate change on water yield in the Upper Wind River Basin. J Am Water Resour Assoc 36:321–336
Tague C, Grant GE (2004) A geological framework for interpreting the low flow regimes of Cascade streams, Willamette River Basin, Oregon. Water Resour Res 40: W043031–W043039
Taylor B (1999) Salmon and steelhead runs and related events of the Clackamas River Basin – a historical perspective. Portland General Electric, Portland
Thornthwaite CW (1955) The water balance. Publ Climatol 8:1–104
Van Katwijk V, Rango A, Childress A (1993) Effect of simulated climate change on snowmelt runoff modelling in selected basins. Water Resour Bull 29:755–765
Wigley TM, Jones PD (1985) Influences of precipitation changes and direct CO_2 effects on streamflow. Nature 314:149–152
Xu CY, Singh VP (2004) Review on regional water resources assessment models under stationary and changing climate. Water Resour Manage 18:591–612
Zimmerman D, Pavlik C, Ruggles A, Armstrong MP (1999) An experimental comparison of ordinary and universal kriging and inverse distance weighting. Math Geol 31:375–390

Editorial responsibility: Gregory Jones, Ashland, Oregon, USA

Submitted: February 9, 2006; Accepted: November 20, 2006
Proofs received from author(s): February 8, 2007